DESIGN AND TEST OF A SMALL SINGLE STAGE TURBINE

HENRY H. DEARING, JR.
ROBERT V. HAYES

M.I.T. Gas Turbine Laboratory
Cambridge 39, Massachusetts
May 16, 1952

Professor Shatswell Ober, Chairman,
Department Committee on Graduate Students
Department of Aeronautical Engineering
Massachusetts Institute of Technology
Cambridge 39, Massachusetts

Dear Sir:

In partial fulfillment of the requirements for the degree of Master of Science in Aeronautical Engineering, we hereby submit a thesis entitled "Design and Test of a Small Single Stage Turbine".

Respectfully,

DESIGN AND TEST OF A SMALL SINGLE STAGE TURBINE

by

Henry H. Dearing, Jr., Lt. Comdr., United States Navy
B.S. in A.E., United States Naval Postgraduate School, 1951

and

Robert V. Hayes, Lt., United States Navy
B.S., United States Naval Academy, 1944
B.S. in A.E., United States Naval Postgraduate School, 1951

Submitted in Partial Fulfillment of the
Requirements for the Degree of
Master of Science

at the

Massachusetts Institute of Technology

May 16, 1952

Signature of Authors_____

_____

Department of Aeronautical Engineering

Certified by _____
Thesis Supervisor

_____
Chairman, Department Committee on Graduate Students

DESIGN AND TEST OF A SMALL SINGLE STAGE TURBINE

ABSTRACT

An investigation was conducted to determine the applicability of the recent work done in the field of large full admission turbine design to the problem of designing a small partial admission turbine.

A single stage axial flow impulse turbine with an outside diameter of four inches was designed and its efficiency calculated by methods which have proved successful in large turbine design. The stage was then manufactured and tested. The test results indicated that the maximum efficiency was within two percent of the calculated efficiency.

During the investigation a simple method of manufacturing small turbine stages was developed and proved successful; a test apparatus suitable for conducting investigations into the effects of tip clearance changes, partial admission, and Reynolds number was designed and built; and a test procedure established.

17316

ACKNOWLEDGEMENTS

The authors wish to express their appreciation for the assistance and cooperation of all those who worked with them during the investigation.

Professor Ernest P. Neumann encouraged us to undertake this work, and it is largely due to his enthusiastic interest and guidance that it was completed. We are especially indebted to him for making arrangements for the use of the D.A.C.L. dynamometer and all the coordination this required. His help, suggestions, and criticism at every stage of progress proved invaluable.

We wish to thank Mr. Robert W. Mann of the Dynamic Analysis and Control Laboratory of the Institute, who designed the dynamometer, for his cooperation and help in adapting our test housing to fit the dynamometer, and for his patient help in using it during the test runs.

The completion of our test program hinged on the manufacture of the turbine wheels, and we are, therefore, most grateful for the help given us in this effort by Mr. Edward Gugger. The overall plan for the machining processes and its ultimate success are due to his imaginative and conscientious efforts. He made all the special tools required, instructed us in every phase of the cutting and milling work, and in the last week of the investigation he rebuilt the damaged shaft and bearing arrangements so that the tests could be completed on schedule.

We also wish to thank Mr. Jan Schnittger for his assistance

in the design of the supersonic nozzle blades; Mr. Gideon Hoffman for balancing the turbine wheel; and Professor Edward S. Taylor for his helpful criticisms during the design of the test housing.

Table of Contents

List of Figures

SYMBOLS

B or b	Blade section dimension in the axial direction
C or c	Blade aerodynamic chord
$C_{1,2}$	Absolute stream velocity
E	Modulus of Elasticity
g	Gravitational constant
h	Enthalpy
I	Moment of inertia
J	Mechanical equivalent of heat
l	Blade length
M	Mach number
P or p	Pressure
s	Blade spacing
T	Temperature
u	Tangential rotational velocity or radial displacement
w	Relative stream velocity
W	Work
α	Air angle
β	Blade angle
δ	Rotor tip clearance
η	Efficiency
μ	Poisson's ratio and viscosity
ξ	Loss coefficient
ρ	Density
ω	Angular rotational velocity

SUBSCRIPTS

A	Annular
L	Loss
O	Stagnation condition
P	Profile
R	Rotor
s	Secondary
S	Stator
st	Stage
t	Turbine
o	Inlet to stator
1	Inlet to rotor
2	Exit from rotor
x	In the axial direction
u	In the tangential direction

I. Introduction

The introduction of the guided missile into the military picture of today has brought with it a demand for small auxiliary power generating units of simple, rugged construction and high output. For some applications the gas-driven turbine appears to offer an especially attractive answer. In one of its simpler forms this unit consists of a combination storage and combustion chamber for a solid fuel, one or two simple nozzles, and a single stage turbine which is driven by the gaseous combustion products of the fuel.

Such units have been successfully designed in the past where work output requirements have been moderate compared to the energy available in the fuel supply. Recent requirements for much higher output per unit weight and volume of the power generating unit have forced the re-examination of the problem of designing small partial admission turbines.

The art of designing full admission gas turbines has made rapid strides since the advent of the turbo-jet power plant for aircraft, reliable methods for computing the efficiency of these turbines have been developed, and some work on partial admission performance done by Kohl, Herzig, and Whitney of the National Advisory Committee for Aeronautics (1).

To examine the applicability of the recent work done on large full admission turbine design to the field of small

partial admission turbines a four inch diameter turbine stage was designed and built and its full admission efficiency calculated. The stage was then tested in a specially designed housing and its output and efficiency measured. Provision was also made for future partial admission investigations.

II. Design of the Stages

The design of the turbine stages was divided into two parts, one for a stage with completely subsonic flow and one for supersonic flow leaving the stator but with subsonic relative flow entering the rotor.

Once the decision to use an impulse wheel had been made the design of the stage was largely dictated by the capacity of the machine tools available. With the blade height limited to a maximum of 0.500 inches and the blade passage at the root fixed at a minimum of 0.125 inches a passage designed to produce an air turning angle of 100 degrees with minimum two-dimensional losses was laid out according to a design formula developed by Zweifel (2). The blade section generated by this passage was modified as indicated in Figure 1 by replacing the pointed leading edge with a fitted circular arc. This resulted in a considerable improvement in aspect ratio with only a slight sacrifice in the optimized solidity, s/c, and produced an aerodynamic shape capable of accepting a much larger range of inlet angles.

By placing Mach number limitations of 0.70 on the relative entering velocity, w_1, to avoid choking of the passage, and of 0.95 on the velocity leaving the stator, c_1, the

FIGURE 1.

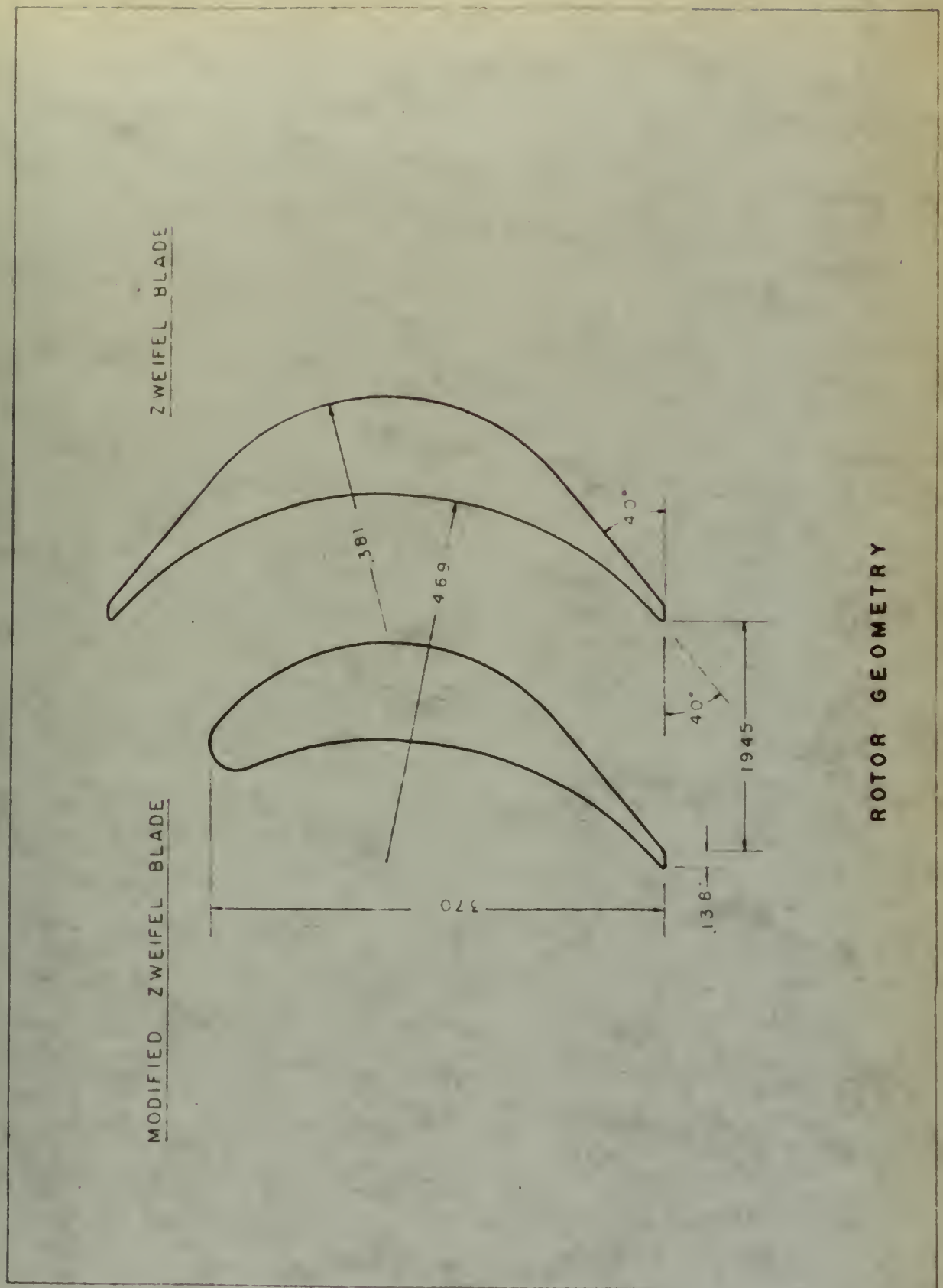
ZWEIFEL BLADE
MODIFIED ZWEIFEL BLADE
.381
.469
40°
40°
1945
.138
370
ROTOR GEOMETRY

velocity diagram for the subsonic stage was completely specified for a back pressure of four pounds per square inch absolute and a total inlet temperature of 530 degrees Rankine.

FIGURE 2

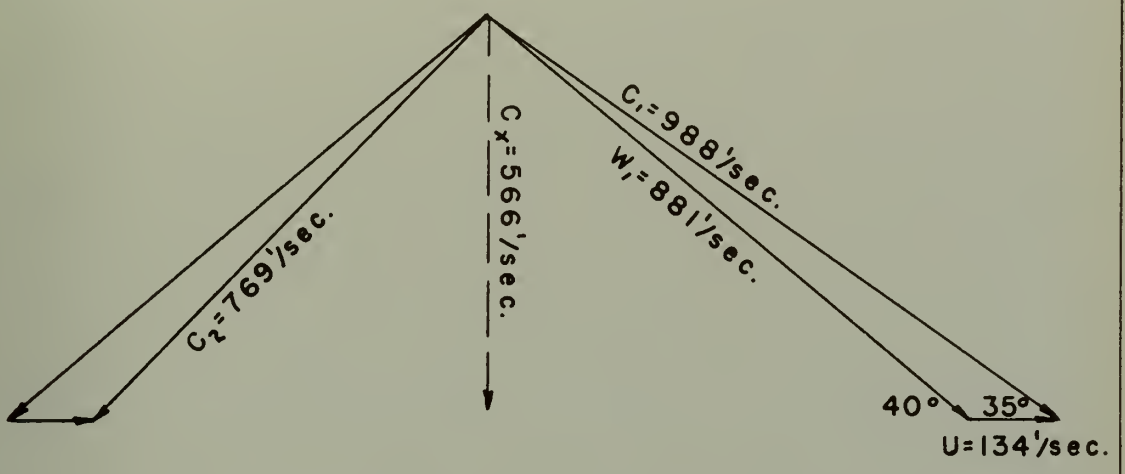

SUBSONIC VELOCITY DIAGRAM.

The trailing edge thickness of the rotor was also limited by manufacturing considerations and once this was fixed at 0.009 inches the number of rotor blades was fixed for the design annulus (four-inch outside and three-inch inside diameters). Continuity considerations in turn set the mass flow.

With a mass flow of 0.438 pounds per second and blade height of the stator equal to that of the rotor the number of stator blades and their trailing edge thickness were likewise specified. The stator geometry was then fixed except for the chord length, chord line curvature, and thickness distribution. The chord length selected represented a compromise between the

requirement for a reasonable aspect ratio to minimize friction losses and the requirement for a large radius of curvature to minimize the possibility of flow separation resulting from too abrupt a turning of the air. The chord line curvature and thickness distribution were designed to conform as nearly as possible to current practice in the aircraft gas turbine field. The subsonic stage geometry appears in Figure 3.

The supersonic stator was designed to operate with the same rotor. The smallest blade outlet angle capable of being machined by the methods discussed below was believed to be of the order of 20 degrees, so with axial air inlet specified the blade turning angle was then limited to about 70 degrees. To achieve an air turning angle of 70 degrees the blade outlet angle was designed for 17.3 degrees to allow for the expansion of the air leaving the stator at a Mach number of 1.133 to an angle of 20 degrees.

The velocity diagram for the supersonic stage operating at a

FIGURE 4

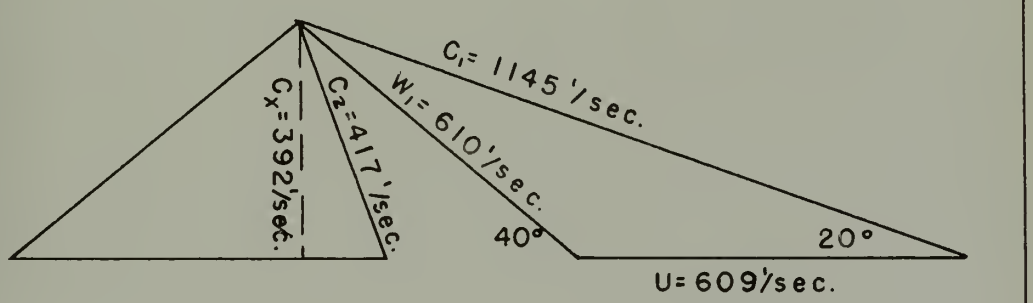

SUPERSONIC VELOCITY DIAGRAM

FIGURE 1.

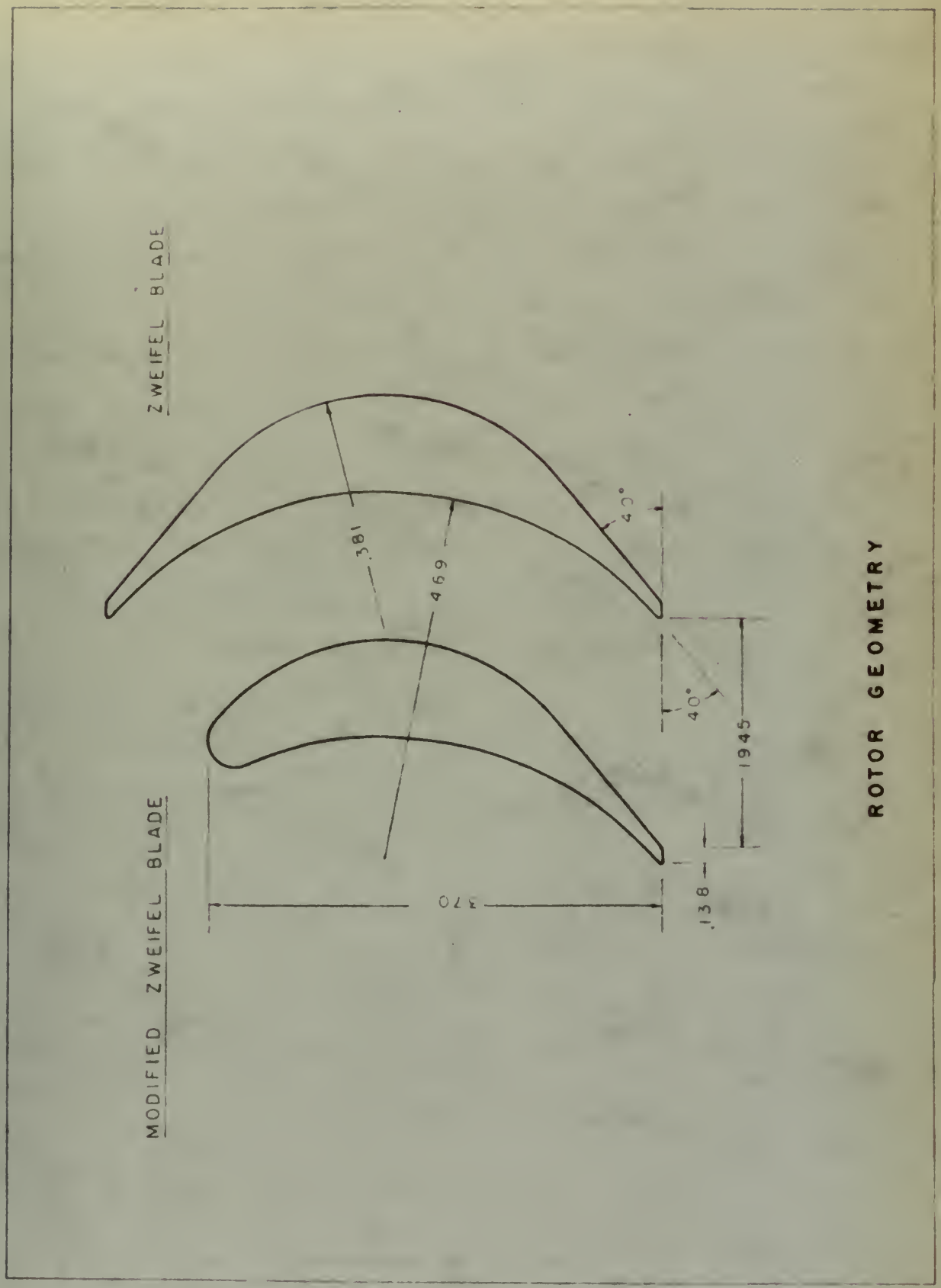
ZWEIFEL BLADE
MODIFIED ZWEIFEL BLADE
.381
.469
40°
40°
1945
.138
.370
ROTOR GEOMETRY

back pressure of four pounds per square inch absolute and a total inlet temperature of 530 degrees Rankine appears above.

As was the case for the subsonic stage, once the blade height of the stator was fixed and the mass flow specified, the number of stator blades and their trailing edge thickness were uniquely determined. And again, except for the chord length, chord line curvature, and thickness distribution, the geometry of the stator was fixed. The chord length was selected to meet the same requirements that applied in the case of the subsonic stator, and the chord line curvature and thickness distribution were selected to fix the nozzle throat at the passage outlet. The blade section was designed with the assistance of Mr. Jan Schnittger of the STAL, Finspong, Sweden. The geometry for the supersonic stage appears in Figure 5.

A discussion of the stresses and radial displacements in the turbine wheel and blades is contained in Appendix I.

FIGURE 5.

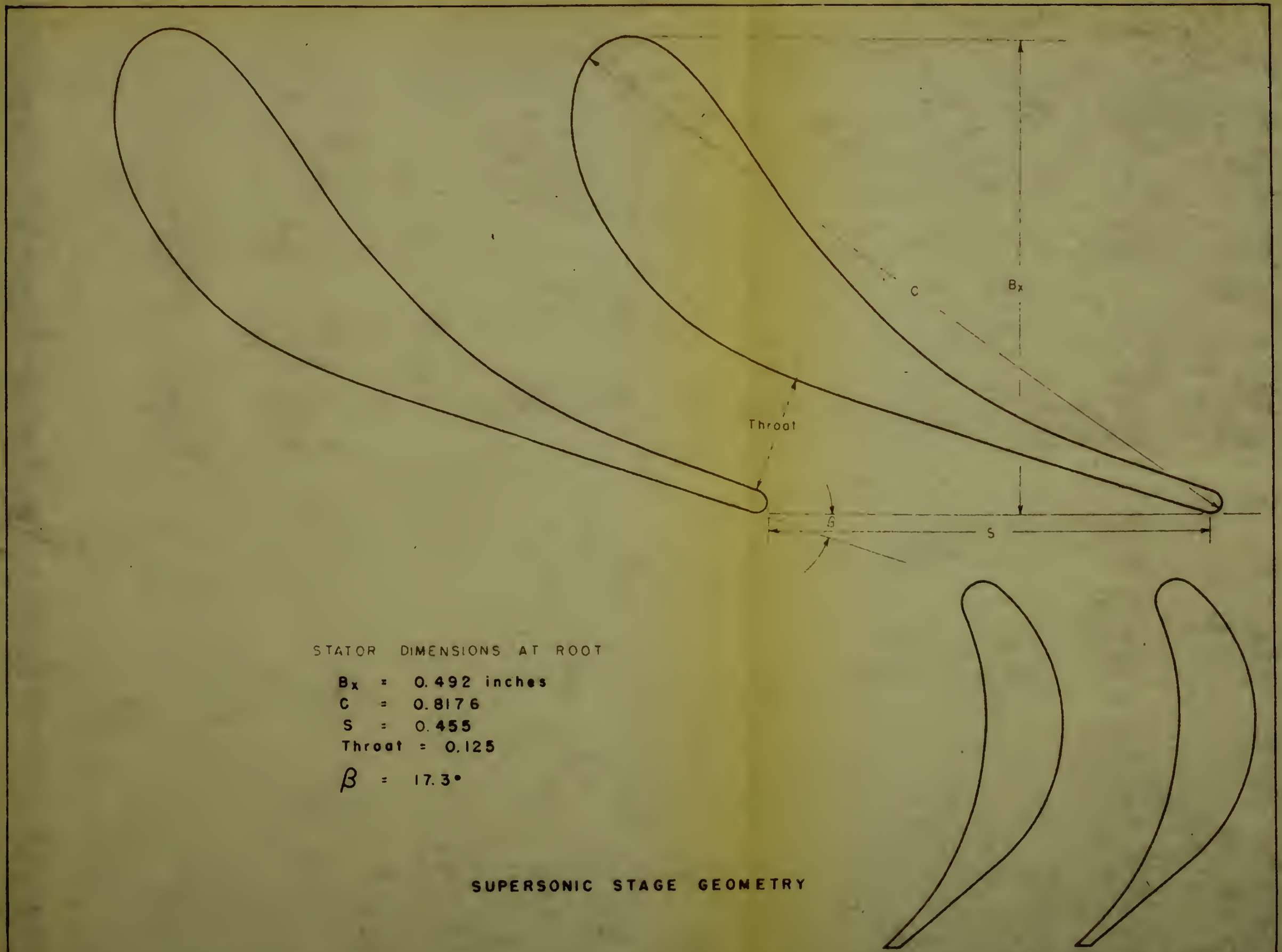

STATOR DIMENSIONS AT ROOT

B_x = 0.492 inches
C = 0.8176
S = 0.455
Throat = 0.125
β = 17.3°

SUPERSONIC STAGE GEOMETRY

III. Calculation of the Efficiency of the Stages

The accurate calculation of the efficiency of a turbine stage depends to a large extent on how precisely the losses in the stage can be predicted. Present practice in gas turbine design is to express these losses in terms of separate loss coefficients for the stator and rotor.

Two methods of computing the loss coefficients, ξ_R and ξ_S, from the stage geometry and the gas properties have been summarized by Van Le (3).

The first of these is due to C. R. Soderberg. His method involves the application of correction factors for aspect ratio, Reynolds number, and inlet angle to nominal loss coefficients, which are functions of the air turning angle and generally of blade thickness as indicated in Figure 6. Van Le has suggested the use of two additional correction factors for solidity and "degree of reaction," α_1 / α_2.

The second method of calculating the loss coefficients follows British practice in which the loss coefficient is taken to be the sum of an annular, a profile, and a secondary loss coefficient. The profile loss coefficient is the two-dimensional loss factor and is a function of the air entering and leaving angles, and the solidity, and requires correction for Reynolds number effects. The annular loss coefficient is a function of wall drag and is, therefore, a function of aspect ratio. All other three-dimensional losses including tip clearance losses are

FIGURE 6

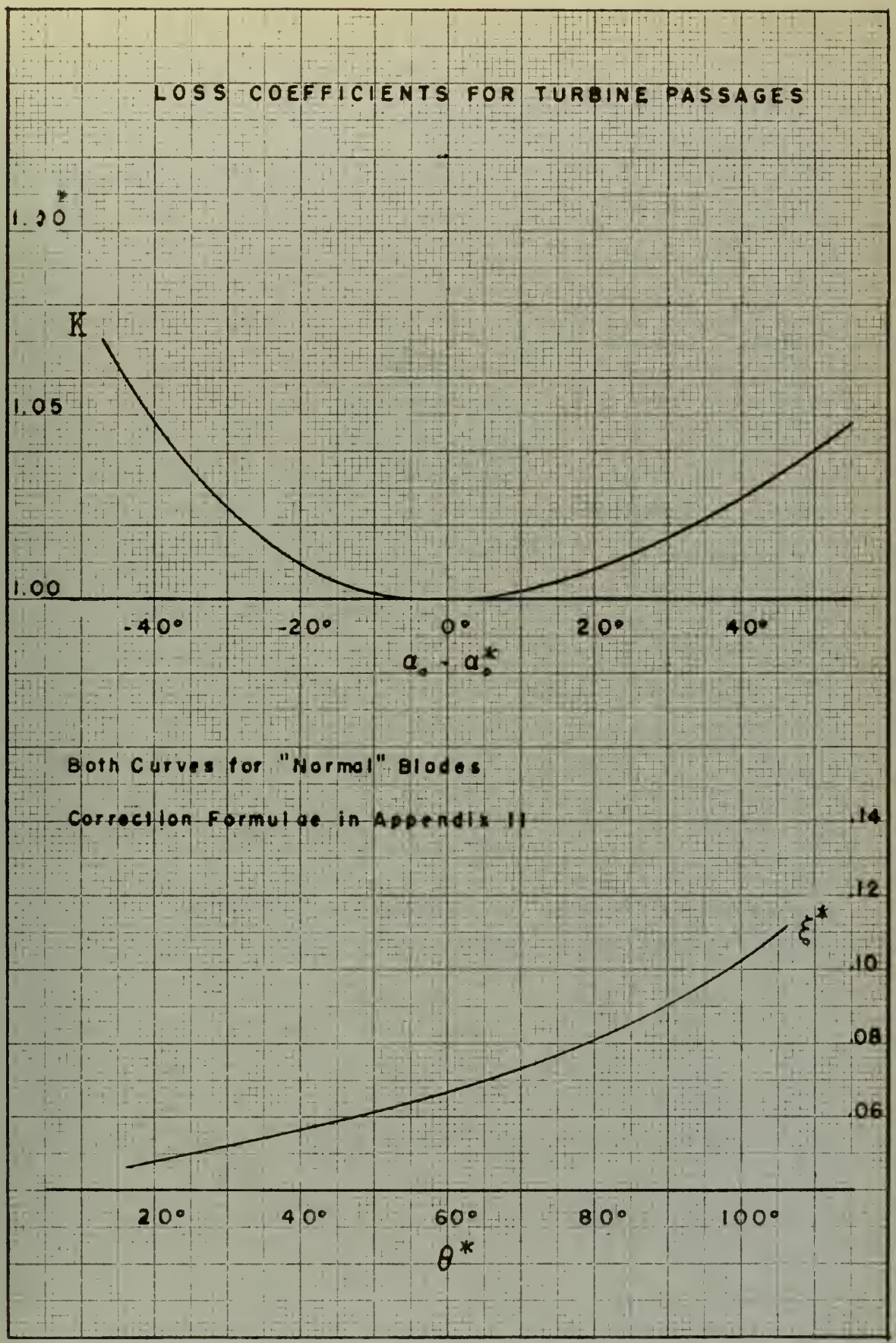
LOSS COEFFICIENTS FOR TURBINE PASSAGES
1.10
K
1.05
1.00
-40°
-20°
0°
20°
40°
$\alpha_o - \alpha_o^*$
Both Curves for "Normal" Blades
Correction Formulae in Appendix II
.14
.12
ξ^*
.10
.08
.06
20°
40°
60°
80°
100°
θ^*

included in the secondary loss coefficient.

The results of the two computations of the loss coefficients are tabulated below. Sample calculations are contained in Appendix II.

Table I

LOSS COEFFICIENTS

Subsonic Stage

	Soderberg		British	
	Rotor	Stator	Rotor	Stator
ξ_P			.0893	.0225
ξ_A			.0150	.0185
ξ_s			.1500	.0256
ξ	.2965	.0934	.2543	.0666

Supersonic Stage

	Soderberg		Van Le		British	
	Rotor	Stator	Rotor	Stator	Rotor	Stator
ξ_P					.078	.0335
ξ_A					.015	.0327
ξ_s					.150	.0053
ξ	.253	.1412	.331	.0146	.243	.0715

The stage efficiency is universally defined

$$\eta_{st} = \frac{\text{actual work}}{\text{reversible work}}$$

Of the several methods of defining reversible work it has been defined here as the work obtained in a reversible expansion from the enthalpy at inlet stagnation temperature to that at exit stagnation pressure.

The turbine efficiency, as distinct from the stage efficiency, has been defined on the basis of a reversible work obtained in a reversible expansion from the enthalpy at inlet stagnation temperature to that at static pressure. This definition, of course, gives lower efficiencies, and is included here for comparison with efficiencies obtained, for example, in auxiliary power generating units where the kinetic energy leaving the stage is not available for useful work.

From the temperature (enthalpy)-entropy diagram, Figure 7, the losses in the rotor and stator are seen to be $h_2 - h_{2s}$, (Δh_{LR}), and $h_1 - h_{1s}$, (Δh_{LS}) respectively. The loss coefficients discussed above have been defined by the relations

$$\xi_R = \frac{\Delta h_{LR}}{w_2^2/2gJ}$$

and

$$\xi_S = \frac{\Delta h_{LS}}{c_1^2/2gJ}$$

The stage efficiency can then be written

$$\eta_{st} = \frac{W_x}{W_{Rst}}$$

$$= \frac{h_{oo} - h_{o2}}{(h_{oo} - h_1) + (h_1 - h_{1s}) + (h_2 - h_{2s}) - (h_{o2} - h_2)} \qquad (1)$$

where the assumption is made that $(h_2 - h_{2s}) = (h_{1s} - h_{2s})$. The error introduced here is of the order of about three percent in this term.

Noting further that

$$h_{oo} = h_1 + C_1^2/2gJ$$

and

$$h_{o2} = h_2 + C_2^2/2gJ$$

the stage efficiency can then be written

$$\eta_{st} = \frac{1}{1 + \dfrac{\xi_s (C_1^2) + \xi_R (w_2^2)}{C_1^2 - C_2^2}} \qquad (1a)$$

The turbine efficiency can be defined in similar fashion

$$\eta_t = \frac{C_1^2 - C_2^2}{C_1^2 + \xi_s (C_1^2) + \xi_R (w_2^2)} \qquad (2)$$

FIGURE 7

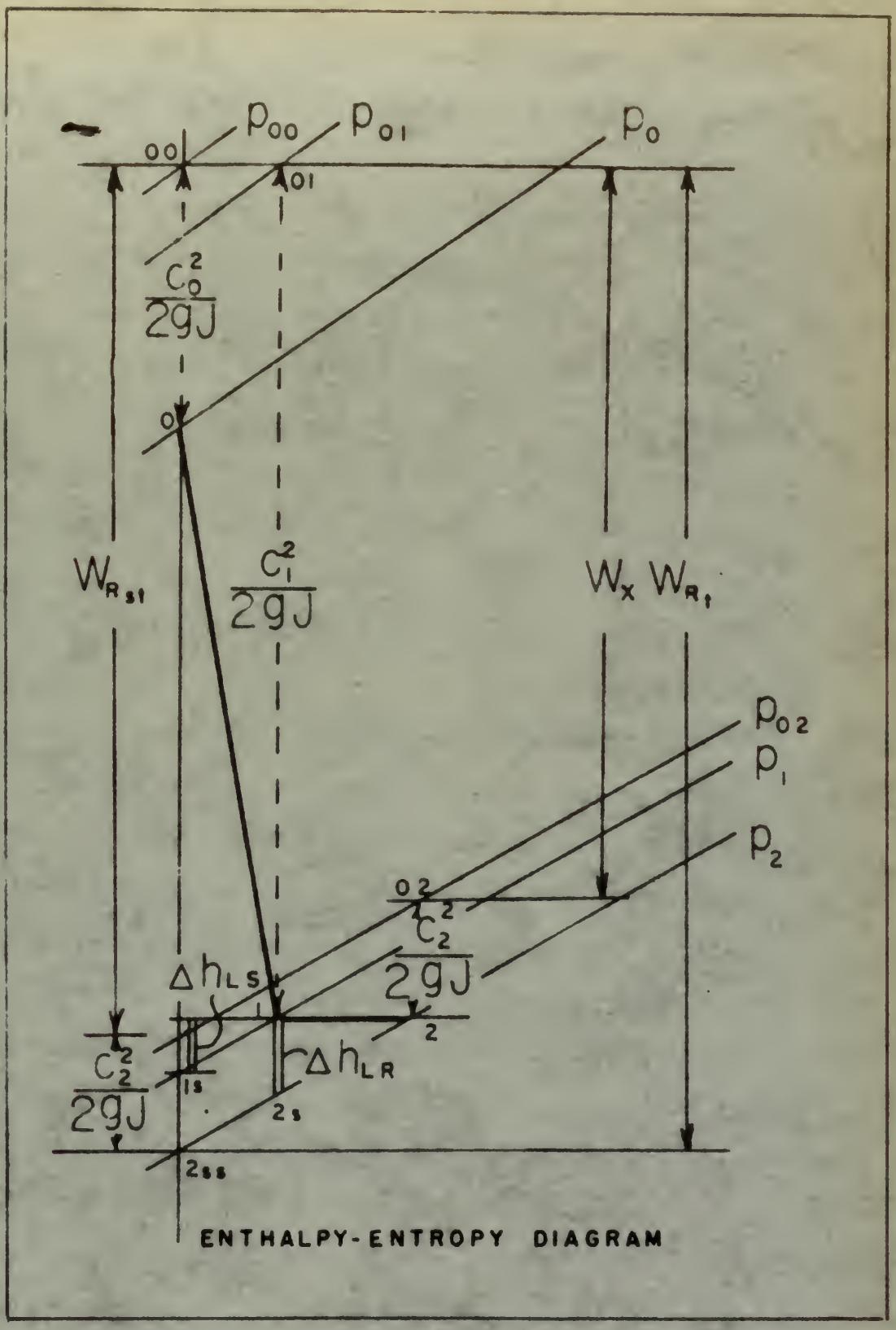
H
S
p_{00}
p_{01}
p_0
00
01
0
$\frac{C_0^2}{2gJ}$
$W_{R_{s1}}$
$\frac{C_1^2}{2gJ}$
W_x W_{R_1}
p_{02}
p_1
p_2
02
$\frac{C_2^2}{2gJ}$
2
Δh_{LS}
1
$\frac{C_2^2}{2gJ}$
1s
Δh_{LR}
2s
2ss
ENTHALPY-ENTROPY DIAGRAM

Using the loss coefficients calculated by the "British" method in Equation 2 gives a turbine efficiency of 76.0 percent, by Soderberg's method of 71.5 percent, and by Van Le's method of 78.1 percent. The corresponding stage efficiencies are 86.0, 80.3, and 88.8, respectively.

Large turbine practice suggests that some correction be made to the efficiencies calculated by the Soderberg or Van Le method for tip clearance losses. Several methods have been suggested in the literature. Hawthorne (7) suggests that the numerator in Equations (1a) and (2) should be multiplied by 0.96 to allow for "losses due to leakage at the tips and other clearances." Schnittger (8) reports that a 3 percent allowance made in a recent design calculation based on Soderberg's method was justified by subsequent tests. This type of correction is based on the premise that the losses due to tip clearances are essentially a constant percentage of the total losses, provided that the tip clearance-blade length ratio remains between 0.01 and 0.02. Schulock and Jensen (9) report that a more useful parameter is the tip clearance-blade chord ratio, and that the losses are functions of the relative Mach number. For a reaction wheel with the same clearance ratio they predict a decrease in efficiency of 4.75 percent. Van Le (3) suggests that losses vary with tip clearance-blade length ratio, and that the reduction in efficiency should be 4 percent based on the design clearance. Herzig, Kuhl, and Whitney (1) propose that the losses vary

as the ratio of the theoretical flow through an annulus with a thickness equal to the clearance dimension to the actual flow through the stage. Soderberg (10) agrees in principle and suggests the following form

$$\Delta\eta_{\text{tip clearance}} = \frac{\pi(1+d)\delta}{\pi l d \sin\beta_2} K \qquad (3)$$

where K is approximately 1.0 for unshrouded blades. This gave an efficiency reduction of 2.5 percent.

Due to the inherent difficulties in calculating the tip clearance at the operating condition it was believed that further attempts to refine the calculation of these losses were unwarranted, and the most conservative computed value based on the best estimate of the actual clearance (0.007 inches), given by Equation 3 above, was used.

The calculated turbine efficiency of the supersonic stage was then 69.0 percent according to Soderberg and 75.6 according to Van Le, compared with 76.0 by the British method.

IV. Equipment and Instrumentation

A. Manufacture of the Wheels

The turbine wheel and the two stator rings were manufactured out of Dural aluminum disks using a pantograph engraving machine to cut the blades. When the stage geometry had been designed the blade cross section was drawn to a 16:1 scale, and a template cut by hand to this size out of 1/16 inch sheet brass. This template was then used in the pantograph machine to cut a second template on a 4:1 scale using a 1/2 inch end mill. This second template provided a snug fitting slot for the follower used in cutting the wheel, again using a 4:1 reduction scale, as shown in Figure 8.

The smallest commercially available end mill for cutting the blades was a 1/8 inch diameter mill capable of cutting to a depth of 1/2 inch. As shown in Figure 9, the end mill was mounted in a vertical driving head whose horizontal motion was controlled by the template follower through a four bar linkage. The disk, which had been slotted to relieve the cutter, was held in an indexing head, and the depth of the cut controlled by raising the bed to which the indexing head was mounted.

The blade generated by the milling cutter then had an untwisted, untapered shape with constant cross section, a maximum length of 1/2 inch, and a minimum passage width at

the root of 1/8 inch.

This machining procedure resulted in the reproduction of a blade shape with almost exactly the desired cross section, the error in reproduction being of the order of 1/16th of the error introduced in cutting the initial template. Although the surface of the blade showed evidences of chattering of the cutter, the magnitude of these surface imperfections was not considered sufficiently large to warrant rejection of this method of manufacturing the wheels.

Figure 8. Supersonic Nozzle Blade Templates

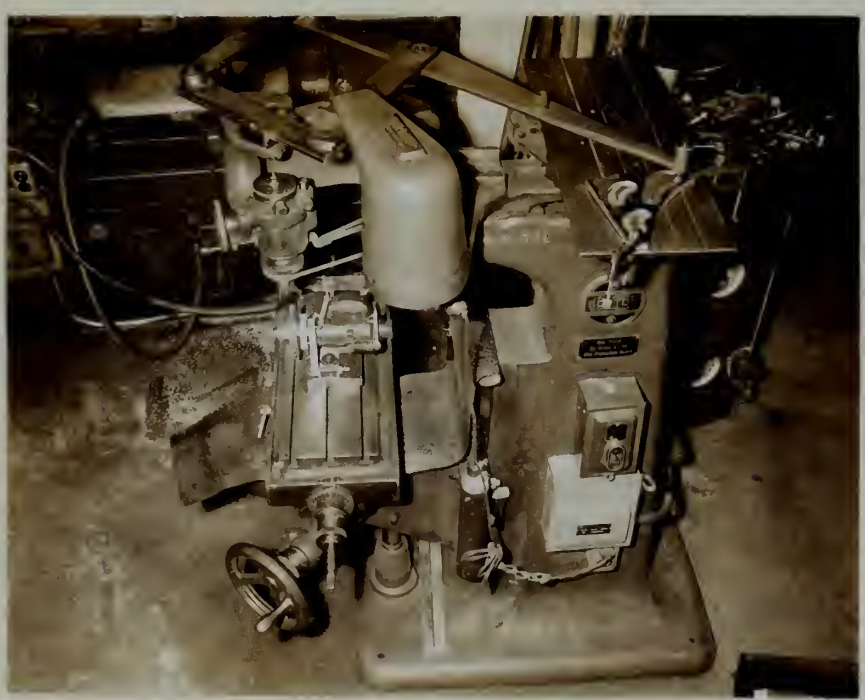

Figure 9. Pantograph Engraving Machine Set Up to Cut the Supersonic Nozzle

B. Design and Manufacture of the Test Housing

In order to test the stages a housing was designed and built by the authors with the assistance of the Boston Naval Shipyard and the Sloan Automotive Shop of the Institute.

Figures 10, 11, and 12 show the housing assembly. It was designed to test stage with outside diameters from 2 1/2 to 6 inches on metered dry air at inlet pressures up to the capacity of the 125 pound air compressor of the Gas Turbine Laboratory and with back pressures as low as 2 pounds per square inch absolute, the capacity of the steam ejector system. A schematic diagram of the air supply system is shown in Figure 13. Provision was made for pressurized oil mist lubrication of the two Barden high speed bearings in the original design, requiring the design of front and back labyrinth seals to equalize the flow of oil vapor forward to atmospheric pressure through the housing and aft into the turbine stage. The oil system was eliminated in the manufactured housing, but the labyrinth system retained, and the bearings were lubricated by hand between test runs. The assembled housing and the dynamometer were rigidly bolted to a common mounting plate to insure positive allignment of the shafts, and the housing outlet was connected to the ejector pipe with a flexible coupling as shown in Figure 14.

The stator assembly is shown in Figures 11, 12, and 15,

and consists of an aluminum nozzle ring into which the stator wheel was shrink fitted. This arrangement was provided so that several stator wheels of the same outside diameter could be tested in one nozzle ring and so that nozzle rings with inside diameters of from 2 1/2 to 6 inches could be used.

Partial admission tests were made possible by the use of partial admission plates which fitted onto the front and rear faces of the stator assembly as in Figure 15 which shows the outlet. The inlet side was essentially similar.

The shaft was mounted in two bearings with the wheel overhung as shown in Figure 19 and the whip speed for this configuration calculated as 201,000 rpm. The details of this calculation are contained in Appendix III.

FIGURE 10

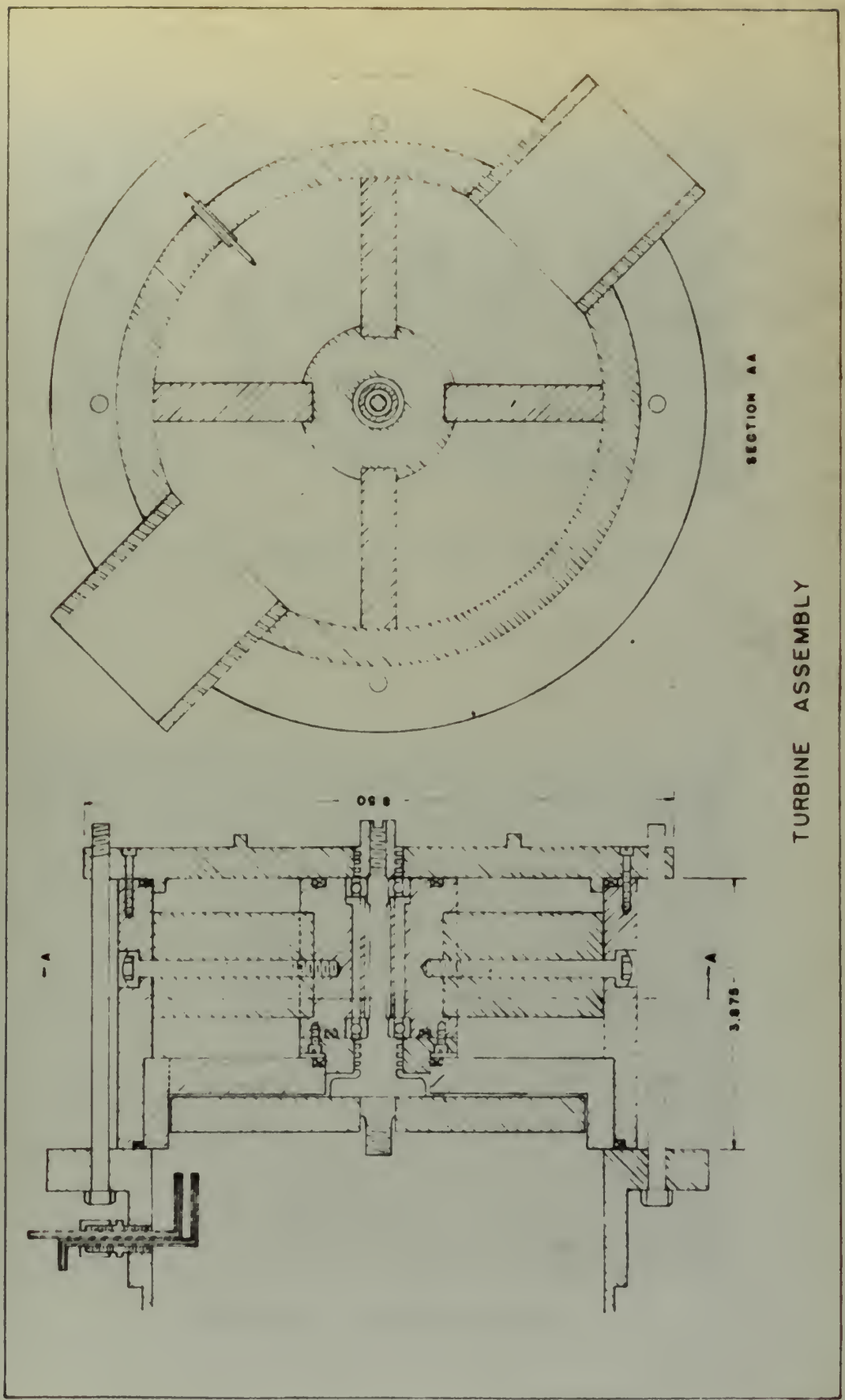

Figure 11. Exploded View of the Test Housing

Figure 12. Assembled Housing

FIGURE 13

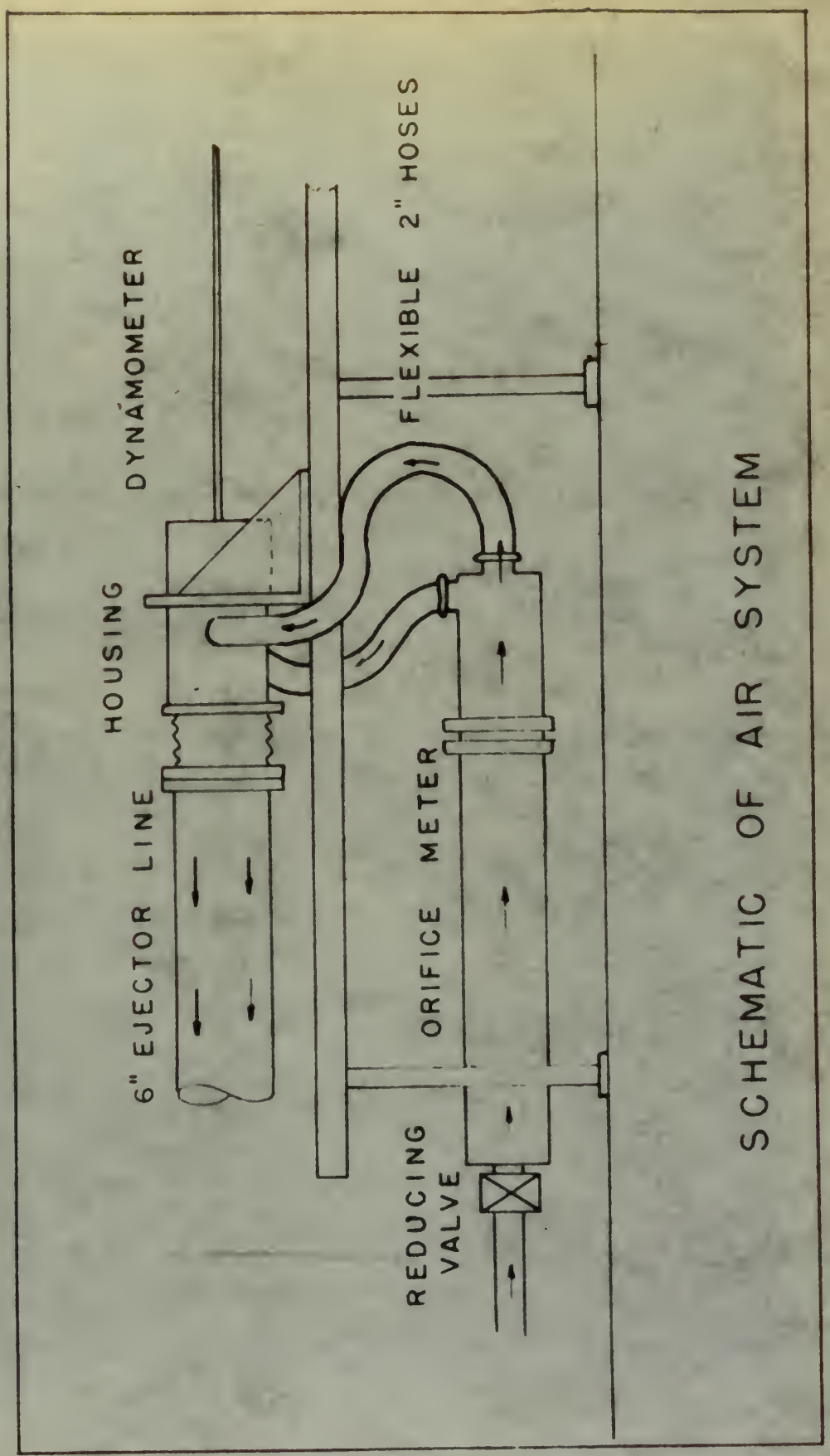
DYNAMOMETER
FLEXIBLE 2" HOSES
HOUSING
6" EJECTOR LINE
ORIFICE METER
REDUCING VALVE
SCHEMATIC OF AIR SYSTEM

Figure 14. Test Housing and Dynamometer Mounted for Test Runs

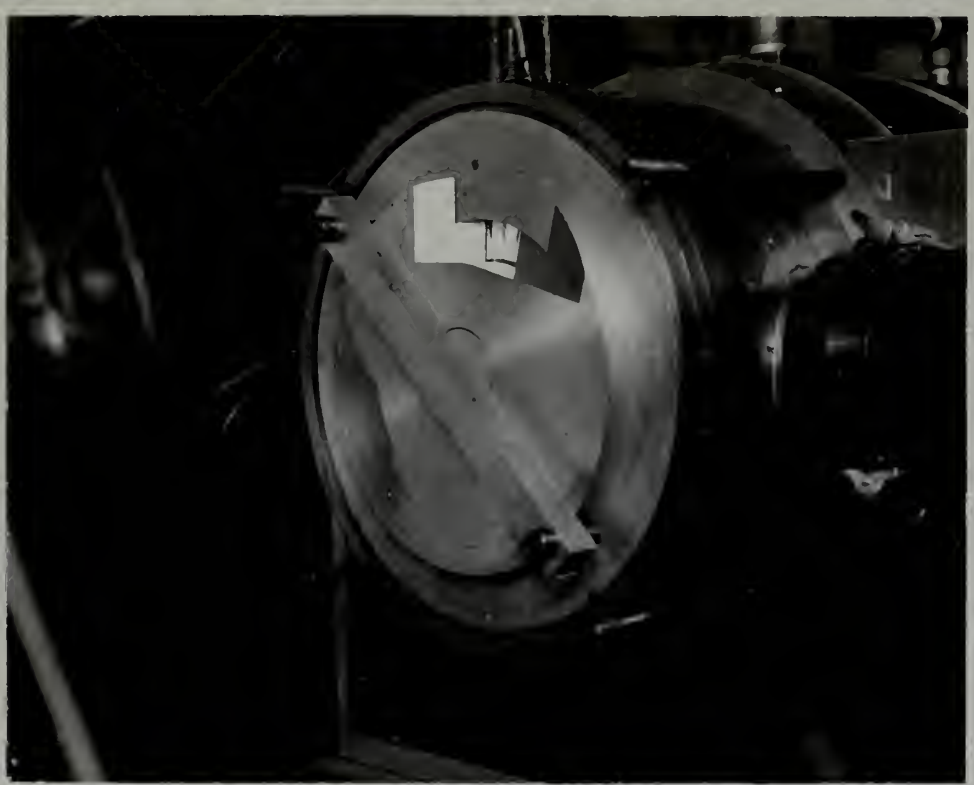

Figure 15. Nozzle Ring with Partial Emission Plate in Place

C. Instrumentation

Instrumentation of the test equipment was divided into three major sections; (1) mass flow measuring instruments, (2) stage pressure and temperature instruments, and (3) torque and shaft speed measuring instruments.

The mass flow of air was measured with an ASME square-edged orifice meter built according to specifications contained in Reference 4.

The minimum requirements for pressure and temperature measurements were considered to be upstream total temperature and pressure, p_{00} and T_{00}, downstream total temperature, T_{02}, and downstream total and static pressure, p_{02} and p_2. Figure 17 shows how these requirements were met. In addition, provision was made for measuring the static pressure between the stator and rotor and at a point well downstream of the turbine outlet. Thermocouples were made according to specifications recommended by Pratt and Whitney Aircraft Corporation (5).

Torque and shaft speed measurements were made with a specially designed dynamometer made available by the Dynamic Analysis and Control Laboratory of the Institute. A description of this piece of equipment is contained in Reference 6.

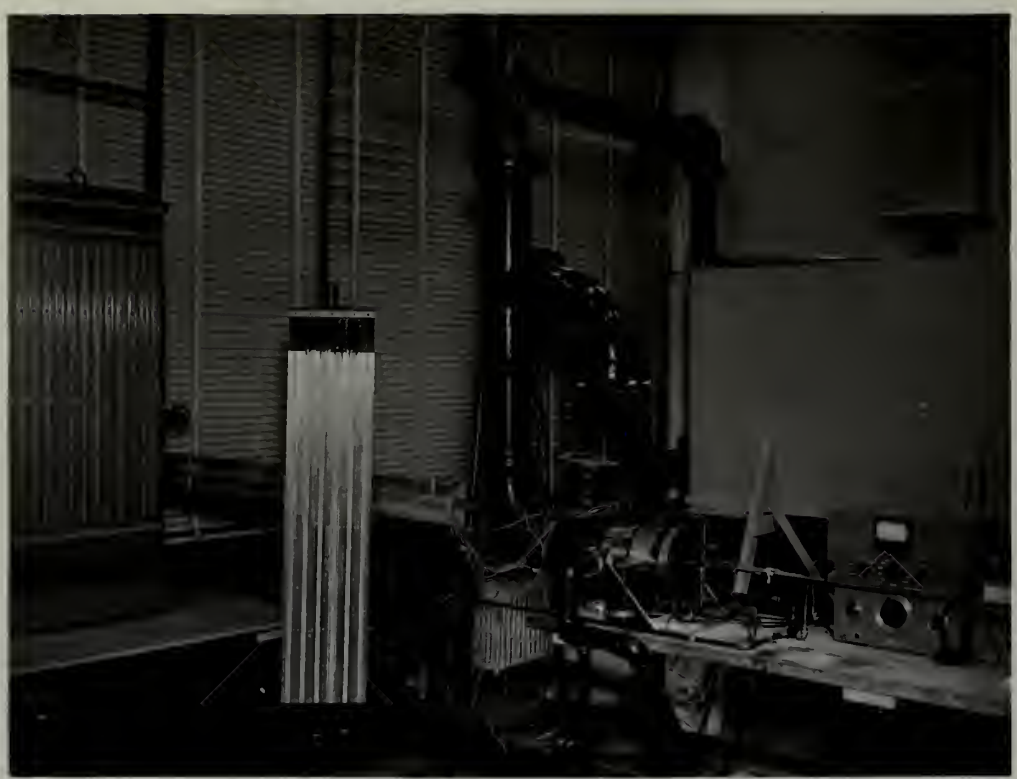

Figure 16. General View of the Test Equipment

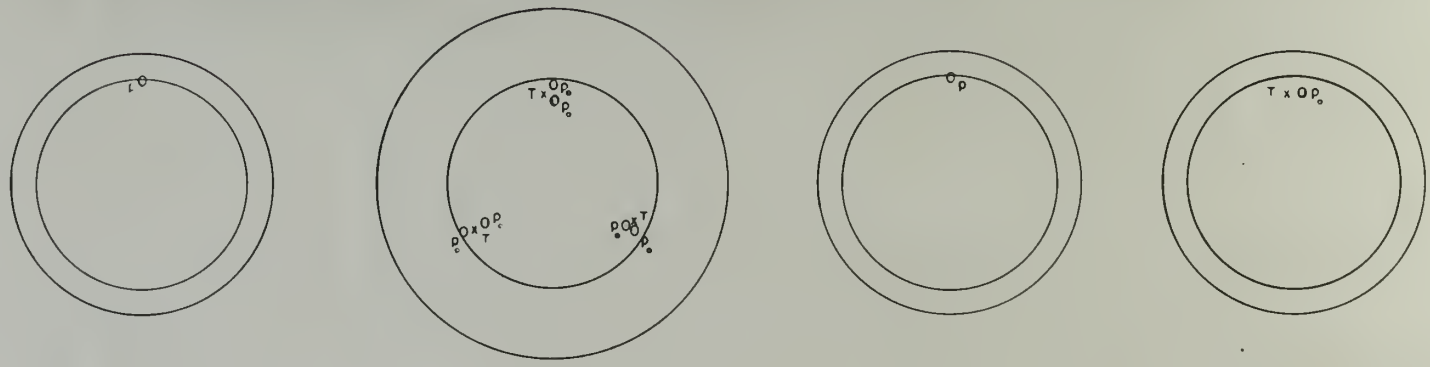

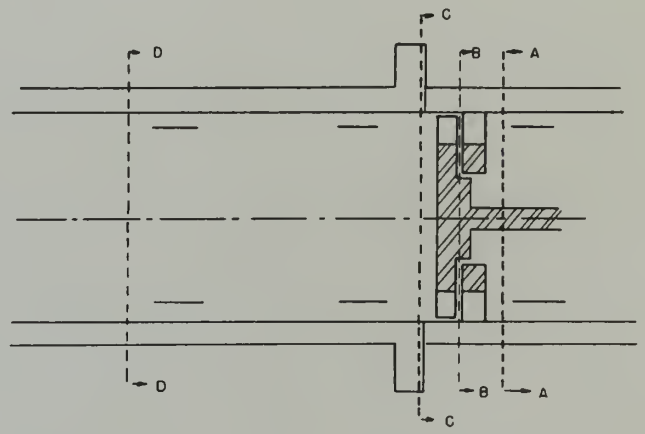

T : THERMOCOUPLE,
P_o TOTAL PRESSURE
P : STATIC PRESSURE

SCHEMATIC OF INSTRUMENTATION SYSTEM

FIGURE 17

V. Test Procedure

The performance of the turbine stage was determined by controlling the inlet and outlet pressures so as to give the designed pressure ratio across the stage. The inlet pressure was controlled by means of a throttle valve connected to a 125 psia air compressor. The air supply was taken from this source so as to reduce the moisture content of the air below that which would cause icing in the turbine stage.

The exhaust pressure was controlled by means of a throttle valve leading to the 6" steam ejector in the Gas Turbine Laboratory. This permitted exhaust pressures as low as 3.00 psia with the mass flow used by the turbine.

The mass flow of air was measured by means of the standard square edged orifice meter, which was placed between the inlet throttle valve and the turbine inlet.

The turbine rpm was controlled by varying the air pressure in the dynamometer casing to give the desired turbine rpm.

With the desired inlet pressure, pressure ratio across the stage, and turbine rpm held constant, the various temperatures and pressures, as shown in Figure 17, were recorded. The pressures were read by means of a mercury manometer board while the temperatures were measured by means of a potentiometer connected to the various thermocouples. At the same time the torque output of the turbine was recorded by measuring the angular rotation of the dynamometer casing and comparing this with a calibration curve of torque versus rotation.

Data was taken at the following operating conditions:

1. Design rpm (P_{o1} at design)
   a) Design pressure ratio
   b) Critical pressure ratio for the nozzle
   c) One pressure ratio above design, P_2 minimum for capacity of ejector
   d) Two pressure ratios below critical

   (These runs were duplicated to check reproducibility of results).
2. RPM 10% below design
   a) Design pressure ratio
   b) Two pressure ratios above critical
   c) Three pressure ratios below critical
3. RPM 10% above design
   a) One pressure ratio at design pressure ratio.

      (Bearing failed at this rpm preventing further runs).

VII Results and Conclusions

When the original turbine efficiencies were calculated it was recognized that the velocities, loss coefficients, and pressure ratios were not altogether consistent. For example, c_1 was calculated on the basis of an isentropic expansion from 8.74 to 4.00 psia, although the loss coefficient calculation showed that the nozzle efficiency was of the order of 95 percent. The relative velocities in the rotor were calculated on the basis that the wheel was pure impulse, while the rotor loss coefficient indicated the presence of some degree of reaction. When the test runs were made, therefore, the back pressure on the stage was appropriately reduced in an attempt to obtain the design pressure ratio across the stator. Subsequent recalculation of the velocity diagram and the associated loss coefficients on the basis of the measured pressure ratios used during the tests showed that the new velocities and loss coefficients changed the calculated efficiency by less than one percent. This conclusion was confirmed by the relatively flat characteristic of the curve of η versus u/c near the design point.

Two sources of data for measuring the work output of the turbine were available, the dynamometer and the thermocouples. Some difficulty was encountered in using the thermocouples, since there was an apparent tendency for the readings at any operating point to decrease with time. This indicated the possibility that the shield was introducing varying radiation

errors until it cooled to near stream temperature. During the longest calibration run, however, measurements from the two data sources very nearly coincided, and the thermocouple readings appeared stable. Torque and rpm measurements on the other hand were consistent and reproducible. For these reasons the data presented is based on the dynamometer measurements alone.

The measurement of the upstream total pressure at only one point was considered justifiable since the circumferential variations of static pressure were of small order. Measurements of the downstream pressure presented some problems, and following the calibration run a static pressure tap was placed well downstream in the ejector pipe (at Section D-D, Figure 17) for recording exhaust pressure, at Mach numbers less than 0.1, to calculate the turbine efficiency. At the start of the two final runs at design speed the six total pressure tubes were yawed until maximum pressures were read when operating at the design condition. The average of these pressure readings was then used in calculating the reversible work to determine the stage efficiency.

Based on the measured mass flow of 0.303 pounds per second, the measured stage efficiency was 78.1 percent and the turbine efficiency was 73.6 percent at the design condition.

Two conclusions may be drawn from this result. First, there appears to be some doubt about the validity of Van Le's contention that the Soderberg loss coefficients require

modification. Without these modifications the Soderberg loss coefficients predict efficiencies very close to those measured, while with them they predict somewhat higher efficiencies comparable to those from the British data. Second, the tip clearance corrections predicted from large turbine data appear unduly high. Schnittger (8) has suggested that these losses might better be considered on the basis of the ratio of the tip clearance to the thickness of the boundary layer in the flow at the blade tips, δ / δ_B. When this ratio is less than unity the losses due to the flow of the low momentum boundary layer fluid through the tip clearance space would probably be negligible. It seems likely that δ / δ_B was near unity in the test setup. The distance measured along a stream line from the fairly sharp corner at the forward outer edge of the stator inlet is 1.25 inches.

The test housing is suitably designed to verify this second conclusion by an investigation of the effects of varying the tip clearance and changing the inlet conditions.

Based on the above, the following method for computing the efficiencies of the supersonic stage resulted in a prediction only two percent in error.

(1) Using the velocity diagram based on the two dimensional geometry of the stage at the mean blade radius and the design pressure ratio, loss coefficients were

computed from the data presented by Soderberg.

(2) The efficiencies were calculated using Equations 1a and 2.

(3) No correction for tip clearance losses was made. The data presented in Figure 18, page 3 , is based on two sets of runs. One point at the design condition, the 90 percent design rpm points, and the 110 percent design rpm point were obtained before the rear bearing failed at 110 percent design rpm (approximately 44,000 rpm). The original 8 mm Barden bearings were replaced with 10 mm Fafnir bearings, and the second set of points at design rpm were obtained. Each pressure ratio point was duplicated, the results were found to agree within less than one percent, and the design point efficiency from the first set was verified. The rear bearing failed again, damaging the wheel and concluding the test portion of this work. The cause of the bearing failures remains undetermined.

As noted in Section III provision was made for future investigations into the effects of partial admission in small turbine stages.

It is believed that basic test procedure outline in Section IV is sound. Control of the upstream and downstream pressures was effective. Placing the inlet throttle valve and the ejector throttle valve so that they can be controlled by one man who can watch the manometer board would save considerable time in taking the data. Total pressure

probes at Section C-C in Figure 17 should be redesigned to provide measureable yaw and radial traversing. This would enable boundary layer thickness estimations and more precise integration of the downstream pressure.

FIGURE 18

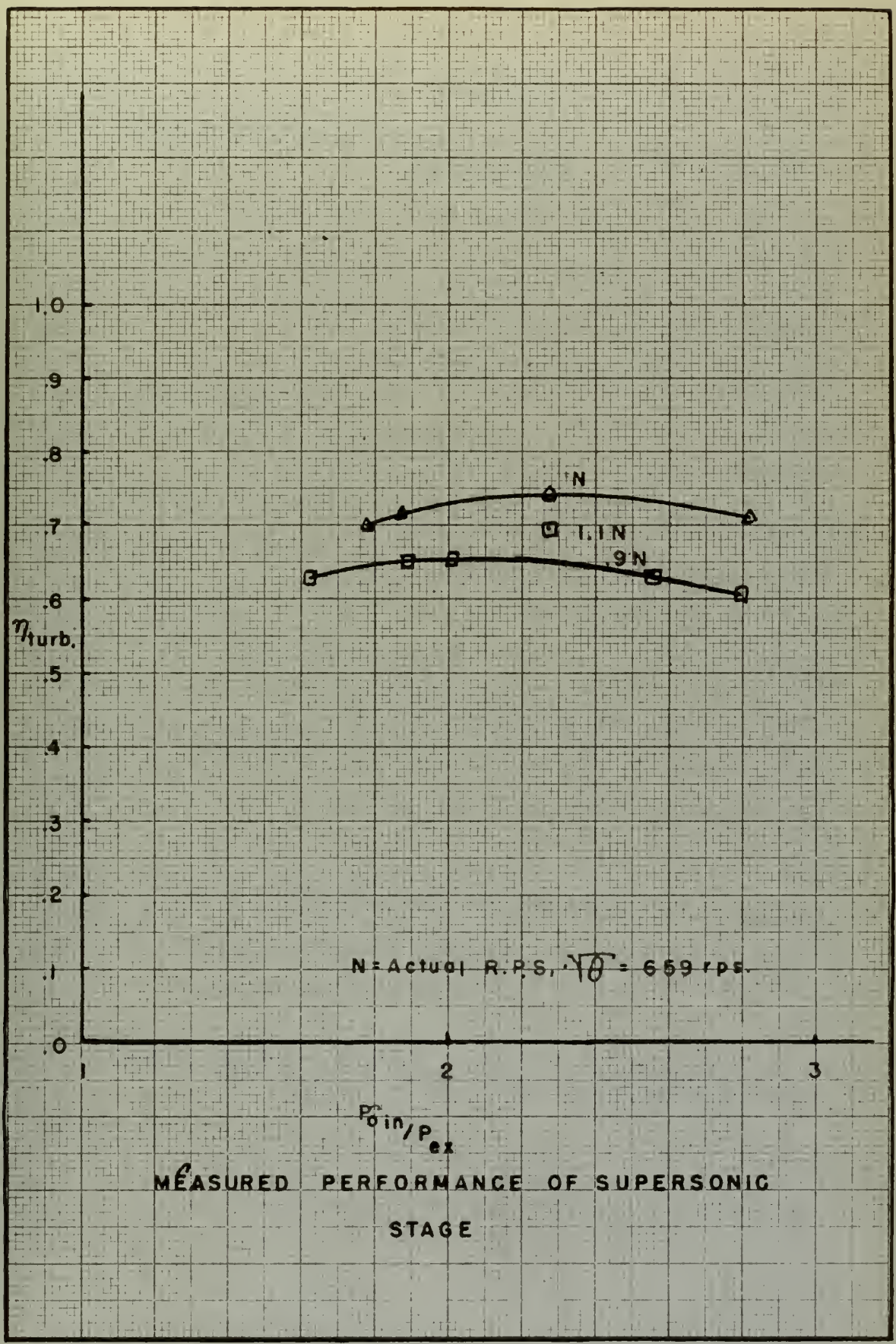

MEASURED PERFORMANCE OF SUPERSONIC STAGE

APPENDIX I

Calculation of the Stresses and Radial Extensions in the Turbine Wheel

The moderate rotational speeds of the turbine wheel indicated that simplifications in the stress and radial displacement calculations could be made. In the following calculations, therefore, the turbine wheel has been replaced by a uniform disk.

Den Hartog (11) has summarized the stress and radial displacement equations for the case of a uniform rotating disk with outside radius, r_o, hole radius, r_1, and without radial loading on either boundary. (Equations 1 and 3 below). Since the actual wheel was made with a sliding fit on its shaft for easy removal, the inner no load boundary condition is identical. By neglecting the blading and calling the radius to the wheel blade tip r_o, the outer boundary condition is also satisfied.

The radial stress was not calculated since it is always smaller than the tangential stress for these boundary conditions. The tangential stress was then

$$s_t = \rho\omega^2 \frac{3+\mu}{8} \left[r_o^2 + r_i^2 + \frac{r_o^2 r_i^2}{r^2} - \frac{1+3\mu}{3+\mu} r^2 \right] \qquad (1)$$

where

ρ = 0.10/386 lb sec^2/in^4

μ = 0.25

r_o = 2.00 inches

r_i = 0.25 inches

evaluated at $r = r_i$ where the stress is maximum

$$s_t = \omega^2 \ (8.45 \times 10^{-4}) \ \text{lbs/in}^2$$

The maximum value for ω^2 anticipated was 17.45×10^6 so that the stress was far from critical.

E. S. Taylor (12) gives the maximum stress for blades of uniform cross section as

$$s = \rho \ \omega^2 / 2\pi 386 \cdot \ \pi (r_o^2 - r_r^2) \qquad (2)$$

and where $r_r = 1.75$ inches

$$s = \omega^2 \ (1.125 \times 10^{-4})$$

The same maximum ω^2 showed that this stress was also far from critical.

The radial extension of the simplified disk was, from Den Hartog

$$u = \rho \omega^2 \ \frac{r}{E} \ \frac{(3 \ \mu)(1 - \mu)}{8} \cdot$$

$$\left[r_o^2 + r_i^2 + (1 + \mu)/(1 - \mu) \ r_o^2 r_i^2 / r^2 - (1 + \mu)/(3 + \mu) r^2 \right] \qquad (3)$$

using $E = 10 \times 10^6$ lbs/in^2

and evaluating at $r = r_o$

$$u = \omega^2 \ (5.74 \times 10^{-11})$$

and with ω^2 again the maximum value, 17.45×10^6

$$u = 0.001 \text{ inches}$$

Since the clearance between the blade tip and the turbine ring could vary from 0.010 to 0.0075 inches without affecting the calculated efficiency of the turbine this extension of the wheel was neglected in the wheel design calculations. The

decision to do this was reinforced by the knowledge that (1) the value of the radial extension, u , calculated was conservatively large due to the simplifying assumptions made above, and (2) the wheel would be chilled in high speed operation and u further decreased by thermal contraction.

APPENDIX II

Calculation of Loss Coefficients

A. Soderberg's Method

1. For the supersonic stator

From Figure 6 for θ^*, the design turning angle, of 70 degrees

$$\xi^* = .0705$$

To correct for the aspect ratio

$$\xi_1 = (1+\xi^*) \left[.975 + .075\ bx/l \right] \quad -1$$

$$\xi_1 = .125 \quad \text{for } bx/l = 1.015$$

To correct for the Reynolds number which is defined

$$R_e = \frac{\left(\frac{2\ S \sin \alpha_1}{S \sin \alpha_1\ 1}\right) c_1 \rho_1}{g \mu_1} = 61{,}300$$

$$\xi_2 = \left[100{,}000/R_e \right]^{1/4} \xi_1$$

$$\xi_2 = .1412$$

Van Le has suggested that ξ_2 be further modified for the degree of reaction

$$\xi_3 = \left[.0027\ \theta^* - .10/.0086\ \theta^* - .09 \right] (\theta^*/90^\circ - \alpha_1 - 1) + .10 - .0027\ \theta^* + \xi_2$$

$$= .1412 - .1278 = .0134$$

$$\xi_4 = \kappa \xi_3$$

where κ for Van Le's data is 1.1

$$\xi_4 = .0146$$

Since the inlet angle is considered the design angle

K from Figure 6 is 1.00, so that

$$\xi_S = K(1+\xi_{2,4}) - 1$$

ξ_S = .1412 (Soderberg)

ξ_S = .0146 (Van Le)

2. For the rotor using the same correction formula

ξ^* = .100

ξ_1 = .182 for bx/l = 1.35

ξ_2 = .253 for R_e = 26,800

and from Van Le

ξ_3 = .3035

ξ_4 = .331

and with K=1

ξ_R = .253 (Soderberg)

ξ_R = .331 (Van Le)

B. British Method

1. For the supersonic nozzle

ξ_{p_1} = .0335 from a curve of ξ_p versus S/C, $\alpha_1 = 0$, contained in Reference 3.

To correct for Reynolds number which is defined

$$R_e = (\rho VC/\mu)_{outlet}$$

R_e = 186,1000

$$\xi_p = \xi_{p_1}(700{,}000/R_e)^{.12}$$

ξ_p = .0335

$\xi_A = .02/AR$

= .0327 for AR = C/l = .611

$$\xi_s = .04\,(1\ \alpha_1/\alpha_2)\left[2\,(S/C)(\mathrm{Tan}\,\alpha_2)\,\cos^2\alpha_2/\cos\alpha_m\right]^2$$

$= .0053$ for $S/C = .65$ and where the air angles are measured from the axial direction .

2. For the rotor using the same correction formulae

$\xi_{p1} = .0780$ from a curve of ξ_{p_1} versus S/C; $\alpha_1/\alpha_2 = 1$

$\xi_p = .0935$ for $R_\theta = 43{,}750$

$\xi_A = .0150$ for $AR = 1.336$

$\xi_s = .15$ for $S/C = .613$

Appendix III

Calculation of the Static Deflections, Slope and Whip Speed of the Turbine Shaft

The static deflection and slope of the turbine shaft were calculated in the following manner:

a) Constant diameter of .375" assumed from station 1 to station 3

b) Constant diameter of .500" assumed from station 3 to station 4

c) Turbine rotor and lock nut assumed as point loads at their respective center of gravities.

Using the above assumptions and the conjugate beam method of solution, the following deflection and slope were calculated at station 4.

δ_y = .0007 inches

θ = .02895 degrees

The whip speed of the turbine shaft was found by use of the formulas and curves in Reference 13. The same assumptions were used as with the deflection and slope calculations with the disc effect of the turbine rotor taken into account.

The disc effect was found to be equal to:

$$\frac{I_d}{ml^2} \cong D = 1.461$$

Using this value for disc effect the following value was found for the whip speed of the turbine shaft:

$$\frac{\frac{w^2}{3EI}}{ml^2} = 3.35$$

$w^2 = 441,000,000$

$w = 21,000$ radians per second

whip speed $= 3,350$ rps

$= 201,000$ rpm

Figure 19. Turbine Shaft, Bearings and Rotor

References

1. Kohl, R. C., Herzig, H. Z, and Whitney, W. J., "Effects of Partial Admission on Performance of a Gas Turbine", NACA TN 1807.

2. Zweifel, O., "The Spacing of Turbo-Machine Blading, Especially with Large Angular Deflection", Brown Boveri Review, December 1945, p. 436.

3. Van Le, N., "Loss Coefficients in Turbine Passages", Gas Turbine Laboratory, Mass. Inst. of Tech., Special Report, January, 1952.

4. Leary, W. A., and Tsai, D. H., "Metering of Gases by Means of the ASME Square-Edged Orifice with Flange Taps", Sloan Laboratory Report 74.1, Mass. Inst. of Tech., July 1, 1951.

5. Clark, F. W., "Characteristics of Stagnation-Temperature Probes for High-Velocity Gas Streams", Pratt and Whitney Aircraft Report PWA-549, April 20, 1945.

6. Mann, R. W., "Air Absorbtion Dynamometer", Dynamic Analysis and Control Laboratory, Mass. Inst. of Tech, Memorandum, Unnumbered, 1952.

7. Hawthorne, W. R., Lecture Notes, Mass. Inst. of Tech., 1951.

8. Schnittger, J., Personal Communication.

9. Schulock, C., and Jensen, R. C., "Blade Tip Leakage and Aspect Ratio Tests", Ellis Reaction Profile, Elliott Company, T. R. 165, Jeannette, Pennsylvania, April 13, 1949.

10. Soderberg, C. R., Personal Communication.

11. Den Hartog, J. P., Lecture Notes, Mass. Inst. of Tech., 1951.

12. Taylor, E. S., Lecture Notes, Mass. Inst. of Tech., 1951.

13. Green, R. B., "Gyroscopic Effects on the Critical Speed of Flexible Rotors", ASME Transactions, 1948.

Thesis 17316
D185 Dearing
Design and test of a small single stage turbine.